Supporting Information

Mechanism of Ammonia-Borane Dehydrogenation Catalyzed by Shvo's Catalyst

Zhiyao Lu, Brian L. Conley and Travis J. Williams*

Donald P. and Katherine B. Loker Hydrocarbon Research Institute and
Department of Chemistry, University of Southern California,
Los Angeles, California, 90089-1661
travisw@usc.edu

Contents

I. General Procedures

All air and water sensitive procedures were carried out either in a Vacuum Atmosphere glove box under nitrogen (0.5-10 ppm O_2 for all manipulations) or using standard Schlenk techniques under nitrogen. Deuterated NMR solvents were purchased from Cambridge Isotopes Laboratories. Benzene-d_6 and diethylene glycol dimethyl ether (diglyme, J. T. Baker) were dried over sodium benzophenone ketyl and distilled prior to use. Shvo's catalyst was purchased from Strem Chemicals. Ammonia borane (NH_3BH_3, AB) was purchased from Sigma Aldrich. Borazine was synthesized and purified by the method used by Wideman and Sneddon.[1] ^{1}H and ^{11}B NMR spectra were obtained on a Varian 600 spectrometer (600 MHz in ^{1}H, 192 MHz in ^{11}B) with chemical shifts reported in units of ppm. All ^{1}H chemical shifts are referenced to the residual ^{1}H solvent (relative to TMS). All ^{11}B chemical shifts are referenced to a BF_3-OEt_2 in diglyme in a co-axial external standard (0 ppm). NMR spectra were taken in 8" J-Young tubes (Wilmad) with Teflon valve plugs. The NMR tubes were shaken vigorously for several minutes with chlorotrimethylsilane then dried in vacuo on a Schlenk line prior to use.

Safety Note. Extreme caution should be used when carrying out these reactions as the release of hydrogen can lead to sudden pressurization of reaction vessels.

II. Summary Scheme

Scheme S1 summarizes the conclusions mentioned in Schemes 3 and 10 of the main text.

Scheme S1. Mechanistic Proposal.

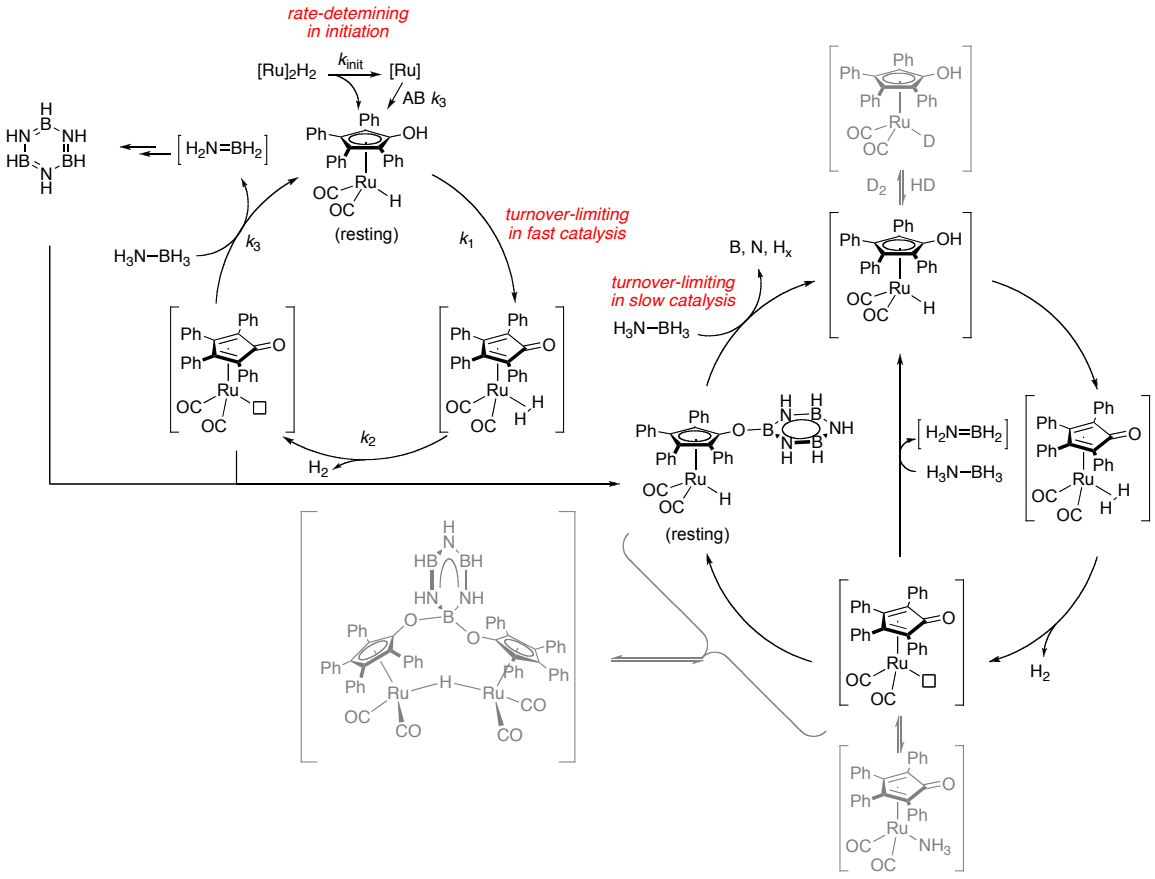

III. Mechanistic Studies Utilizing ^{11}B and ^{1}H NMR Spectroscopy

A. Representative Procedure for Ammonia Borane Dehydrogenation with Shvo's Catalyst.

In a typical reaction, 7.7 mg AB was combined with Shvo's catalyst (**12**, 13.6 mg, 5 mol %) in a 2 mL Schlenk tube equipped with a Teflon stir bar while in a glovebox under nitrogen. The AB concentration and catalyst concentrations may be varied. Diglyme (0.4 mL) and benzene-d_6 (0.2 mL) were added to the tube. The sample tube was immediately inserted into a preheated NMR (70 ˚C) and the kinetic monitoring commenced after quick locking and shimming. Disappearance of AB in the solution was monitored by the relative integration of its characteristic peak in the ^{11}B spectrum (-22 ppm) and the BF_3-OEt_2 standard. All spectra were processed using VNMRJ (v. 2.3). The acquisition involved a 1.67 sec pulse sequence in which 4,096 complex points were recorded, followed by 1 sec relaxation delay. To eliminate B-O peaks from the borosilicate NMR tube and probe, the ^{11}B FIDs were processed with back linear prediction, ca. 5-15 points.

*B. Reduction of **18** with Ammonia Borane.*

In this experiment we show spectra for the reaction in Figure S1.

Figure S1.

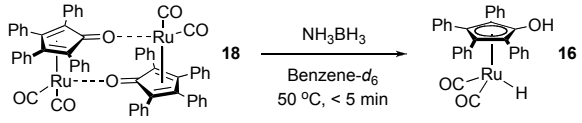

In two J. Young tubes (a and b), 7.7 mg (0.25 mmol) AB and 13.5 mg (5 mol%) **18** were dissolved in 0.6 mL benzene-d_6. A ^{1}H-NMR of tube (a) was taken quickly (ca. 1 min) in a pre-locked and shimmed instrument and some reduction reaction already appears (Figure S2 top). Tube (b) was placed in a preheated oil bath at 50 ˚C for 4 min before quickly taken a ^{1}H-NMR of. The NMR spectrum of tube (b) shows completion of conversion of **18** in this system in 5 min (Figure S2 bottom).

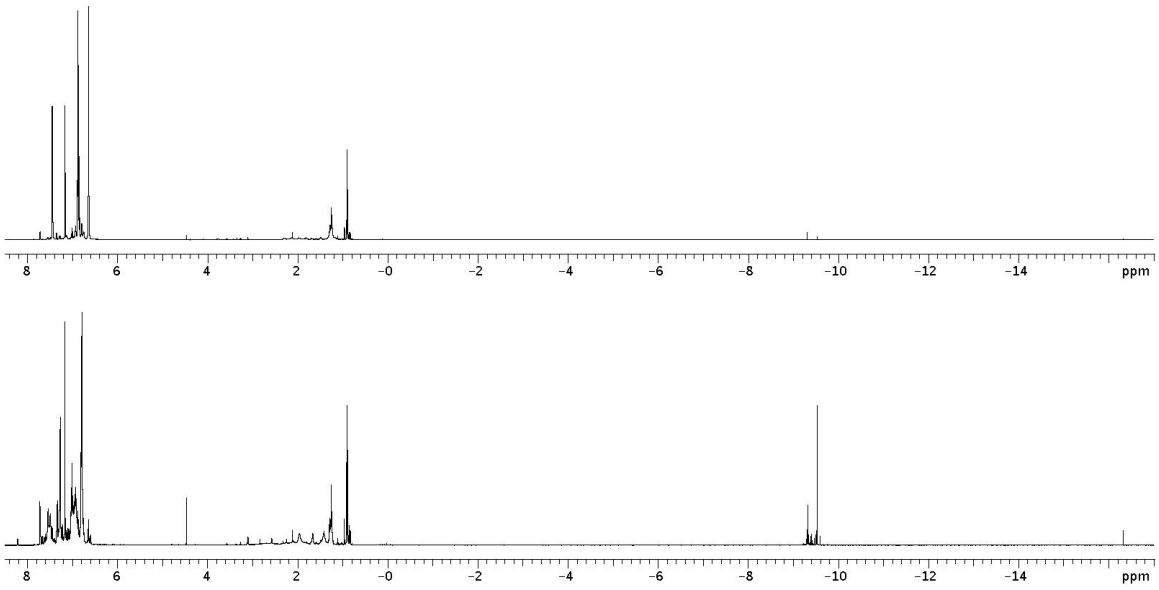

Figure S2. 0.42 M AB with 5 mol% **18** in 0.6 mL benzene-d_6. Top: tube (a) at room temperature in 5 min, some conversion of **18** by AB can be observed. Bottom: in tube (b) **18** is fully reduced to Ru—H hydride species in 5 min at 50 ˚C, suggesting a rate constant $> 10^{-2}$ s^{-1}.

C. Determination of AB and Catalyst Order in Case 3.

These graphs show raw kinetics data fits for [AB] dependence in the slow catalysis case (Figure S3). These correspond to Table 1 in the main text.

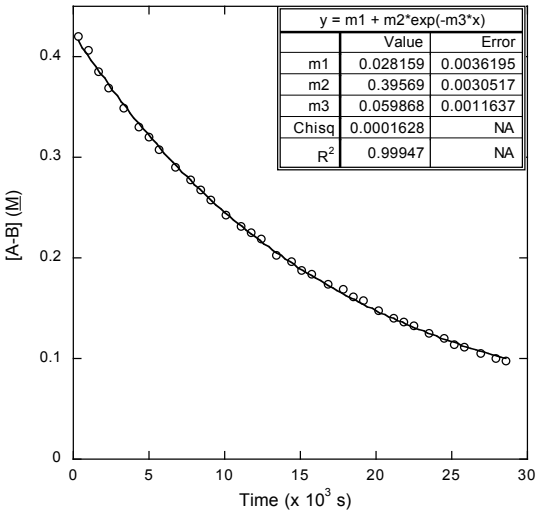

0.42 M AB. k_{obs} = 5.99(12) × 10^{-5} s^{-1}.

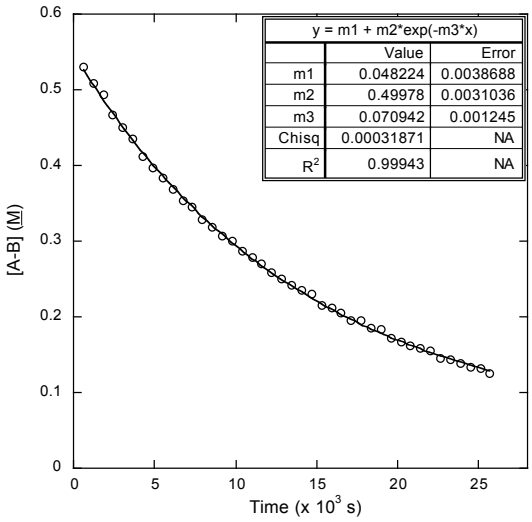

0.53 M AB. k_{obs} = 7.09(12) × 10^{-5} s^{-1}.

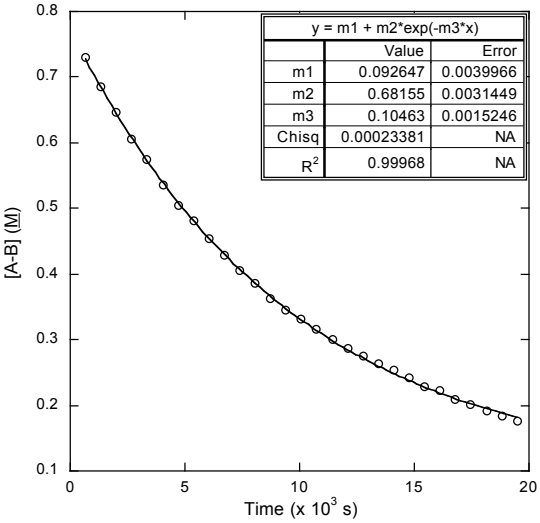

0.73 M AB. k_{obs} = 1.05(2) × 10^{-4} s^{-1}.

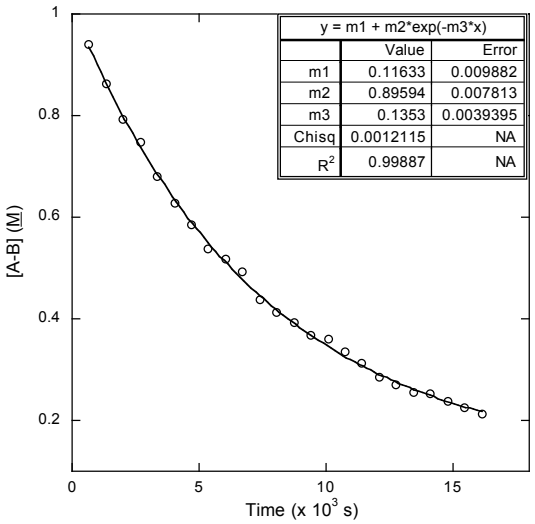

0.94 M AB. k_{obs} = 1.35(4) × 10^{-4} s^{-1}.

Figure S3. [AB] vs. time monitored by ^{11}B NMR in 2:1 diglyme/benzene-d_6 with varying AB concentrations in the slow catalysis case. Exponential coefficients represent the observed rate constants in s^{-1} (× 10^{-3}).

These graphs show raw kinetics data for [Ru] dependence in the slow catalysis case (Figure S4). These correspond to Table 1 in the main text.

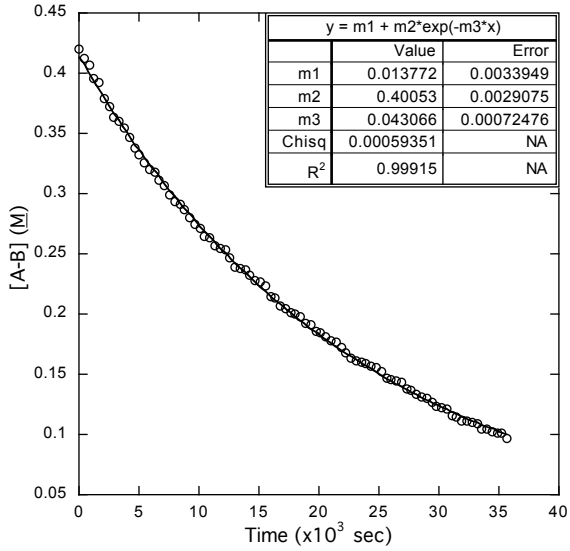

2.5 mol % **12**. k_{obs} = 4.31(1) × 10^{-5} s^{-1}.

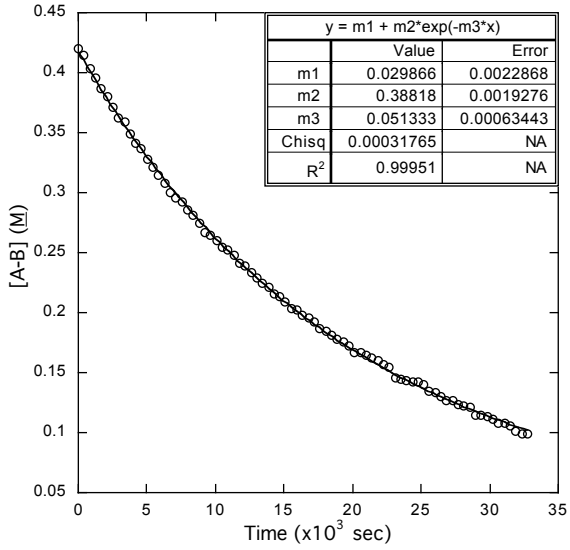

3.75 mol % **12**. k_{obs} = 5.13(6) × 10^{-5} s^{-1}.

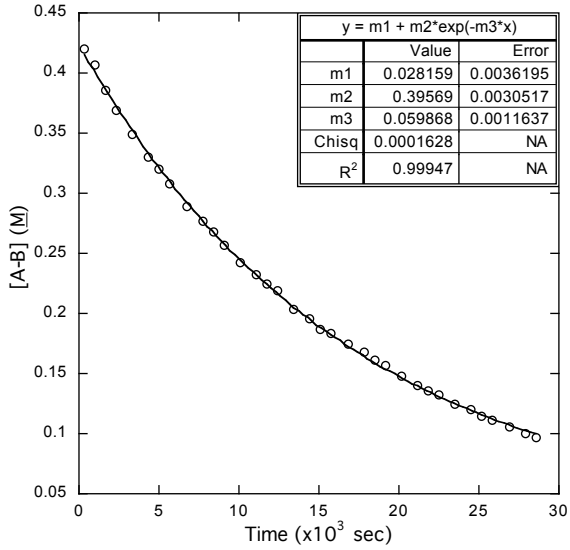

5.0 mol % **12**. k_{obs} =5. 99(12) × 10^{-5} s^{-1}.

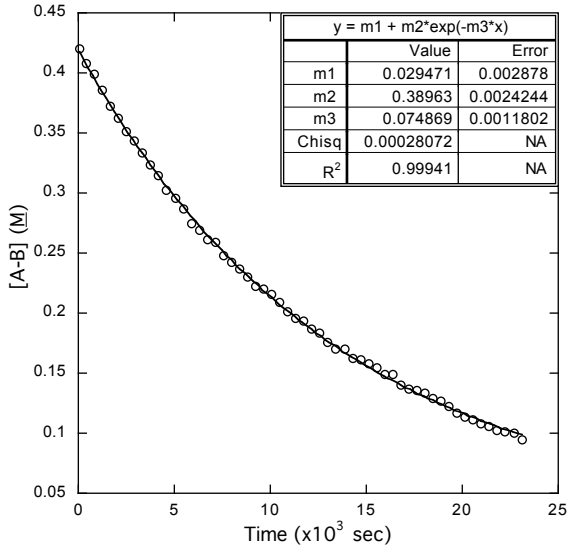

7.5 mol % **12**. k_{obs} = 7.49(12) × 10^{-5} s^{-1}.

Figure S4. [AB] vs. time monitored by ^{11}B NMR in 2:1 diglyme/benzene-d_6 with varying catalyst concentrations in the slow catalysis case. Exponential coefficients represent the observed rate constants in s^{-1} (× 10^{-3}).

D. Kinetic Isotope Effect Experiments and H/D Exchange.

These graphs (Figure S5) show raw data for kinetic isotope effect experiments done on the reaction in case 3.

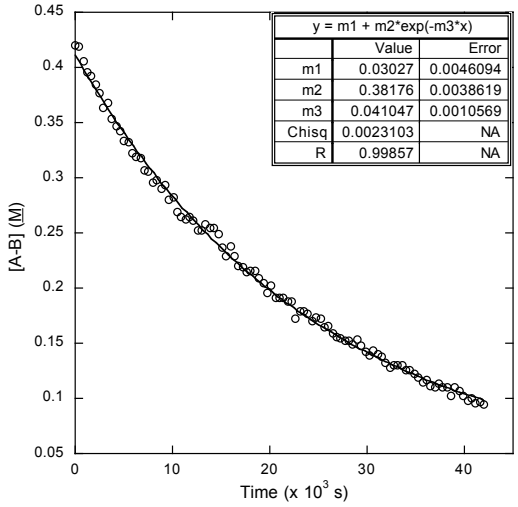

ND_3BH_3, $k_{obs} = 4.10(10) \times 10^{-5}$ s^{-1}
KIE = 1.46(3)

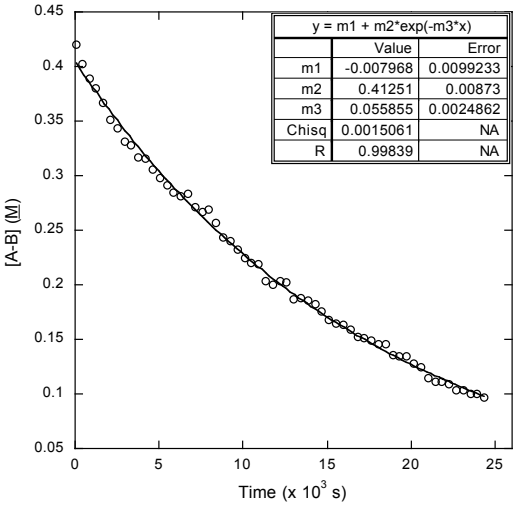

NH_3BD_3, $k_{obs} = 5.59(25) \times 10^{-5}$ s^{-1}
KIE = 1.07(5)

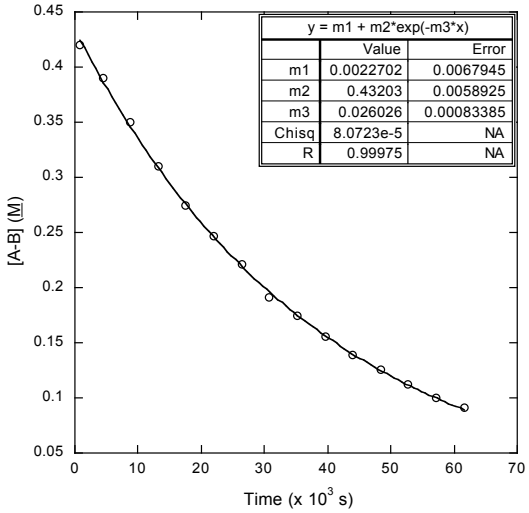

ND_3BD_3, $k_{obs} = 2.60(8) \times 10^{-5}$ s^{-1}
KIE = 2.30(4)

Figure S5. Kinetic isotope effects in dehydrogenation by 5 mol % **12**. And HD signal in ^1H NMR.

Figure S6 illustrates H/D crossover in the course of ammonia borane dehydrogenation.

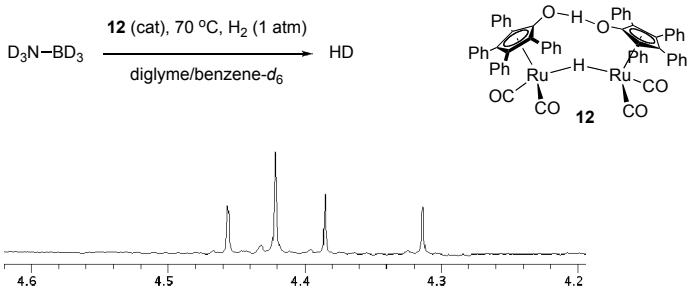

Figure S6. *HD exchange.* ^{1}*H NMR shows* H_2 *and HD in the hydrogen region,* J_{HD} *= 42.4 Hz*

*E. Reaction of Complex **18** with Borazine.*

Figure S7 shows the reaction of **18** with borazine. Figure S7 (middle) shows the hydride region of the ^{1}H NMR spectrum of a benzene solution of **18** in a sealed tube after 1 eq. borazine is added and incubated for 5 min at 25 ˚C. The taller peak in the κ^1-Ru—H hydride region (δ = -9.7 ppm) corresponds to borazine adduct **21**, and the peak in the μ^2-Ru—H hydride region (δ = -18.2 ppm) corresponds to borazine adduct **31**. Multiple κ^1-Ru—H peaks are observed after 2 hours (shown in Figure S7, bottom). The μ^2-Ru—H hydride peak is no longer at presence in the spectrum, and **21**'s peak becomes the tallest in hydride region. Others correspond to other *O*-borylated homologs of **16**, as sketched in Scheme 5 of the main text.

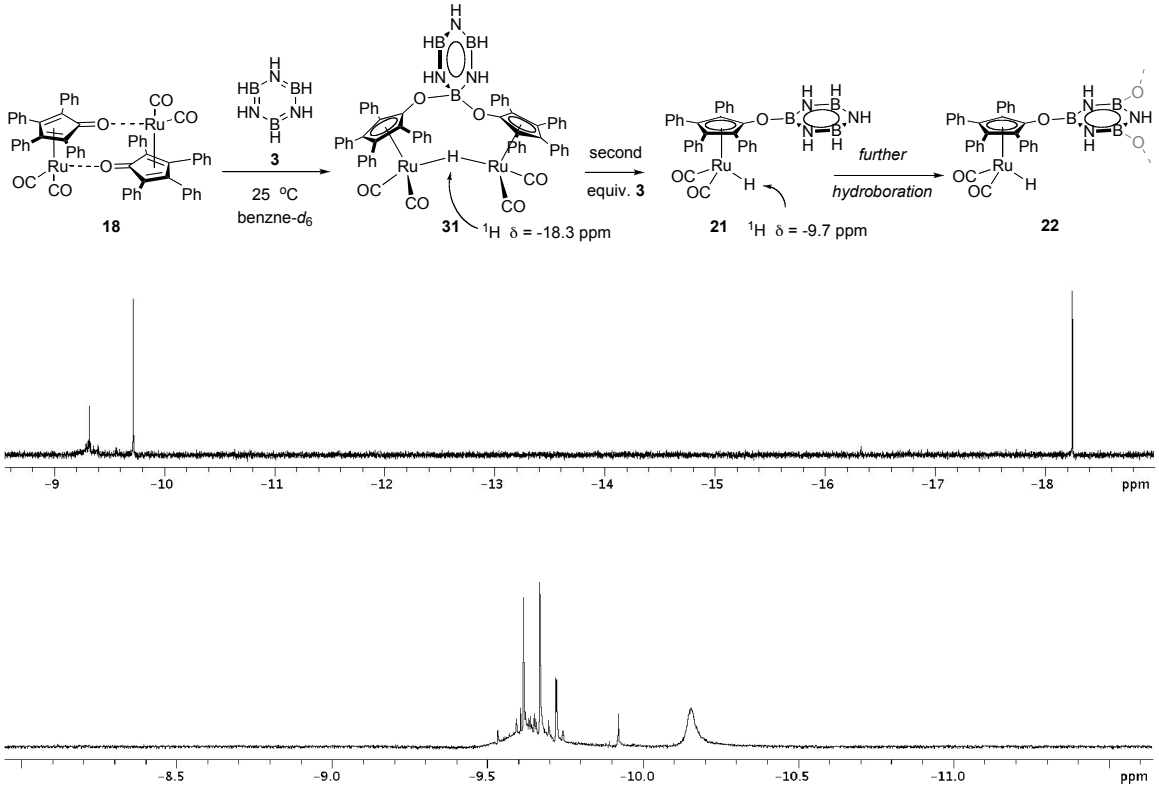

Figure S7. Borazine hydroboration of **18**. Top: scheme. Middle: ^{1}H NMR in 5 min at 25 ^{o}C. Bottom: 2 hours at 25 ^{o}C.

*F. Synthesis and Reactions of **26**.*

26 was prepared *in situ* by a method introduced by Clark[2] as described in the main text. Data treatments for **26**-catalyzed AB dehydrogenation are shown in Figure S8.

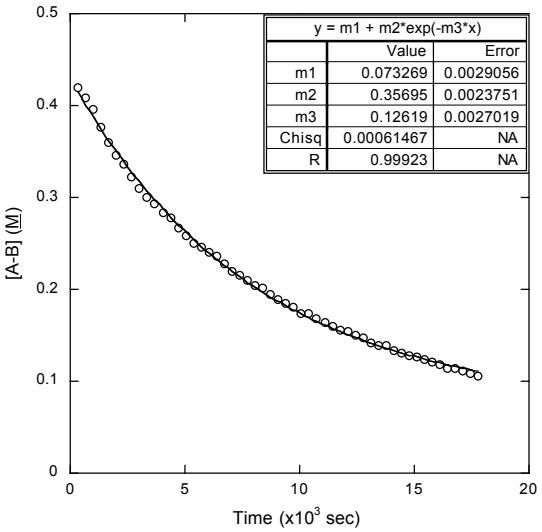

5.0 mol % **26**. k_{obs} = 1.26(3) × 10^{-4} s^{-1}.

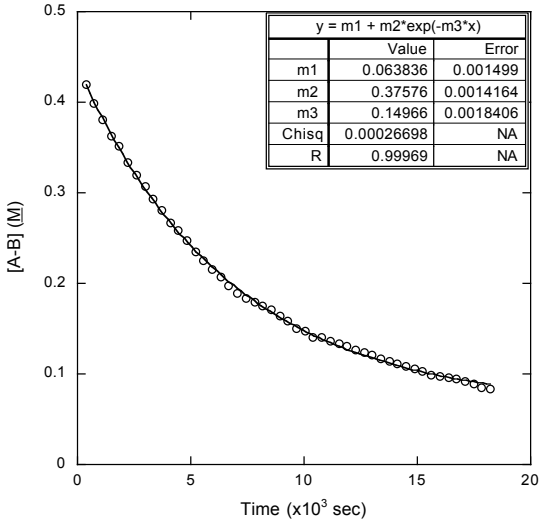

7.5 mol % **26**. k_{obs} = 1.50(2) × 10^{-4} s^{-1}.

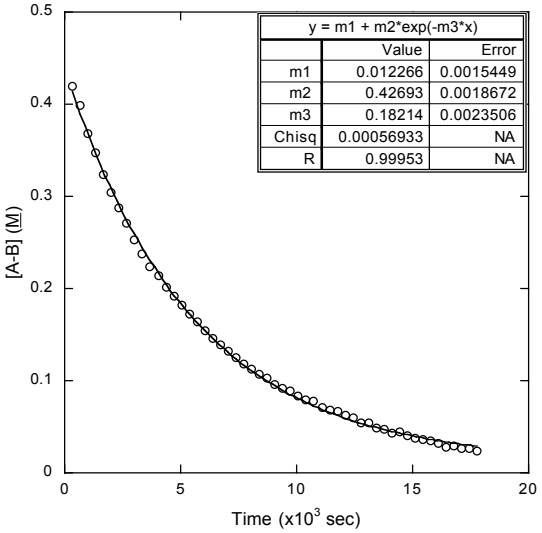

10.0 mol % **26**. k_{obs} = 1.82(2) × 10^{-4} s^{-1}.

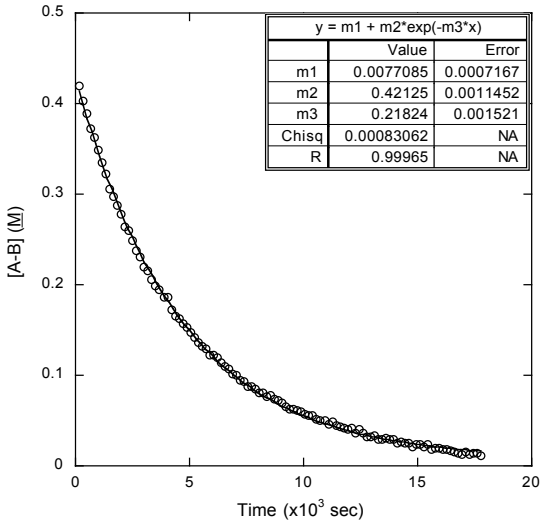

15.0 mol % **26**. k_{obs} = 2.18(2) × 10^{-4} s^{-1}.

Figure S8. [AB] vs. time monitored by ^{11}B NMR in 2:1 diglyme/benzene-d_6 with varying catalyst **11** concentrations. Exponential coefficients represents the observed rate constants in s^{-1} (× 10^{-3}).

G. Ammonia Borane Dehydrogenation in the presence of excess BH_3.

Kinetic experiments in the presence of added BH_3 were conducted as describe in main text. Data fits of these kinetic runs and their control reactions are shown in Figure S9.

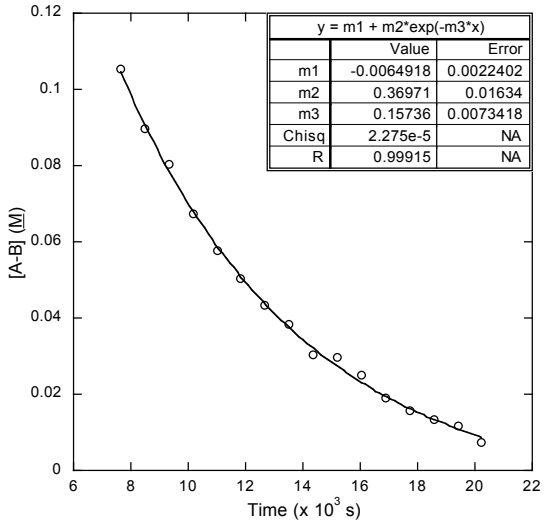

0.5 eq. BH_3·THF. k_{obs} = 1.57(7) × 10^{-4} s^{-1}

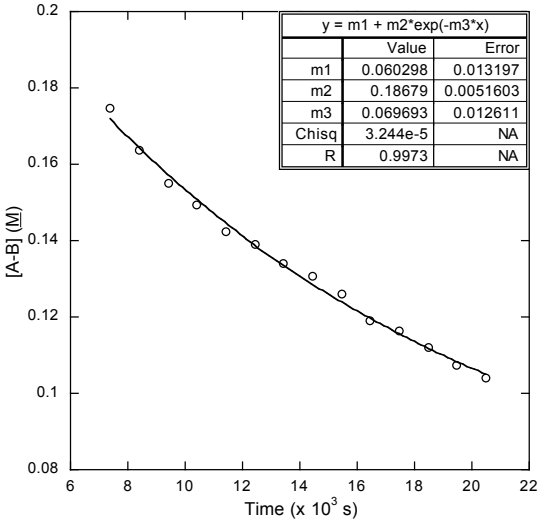

THF only. k_{obs} = 7.0(13) × 10^{-5} s^{-1}

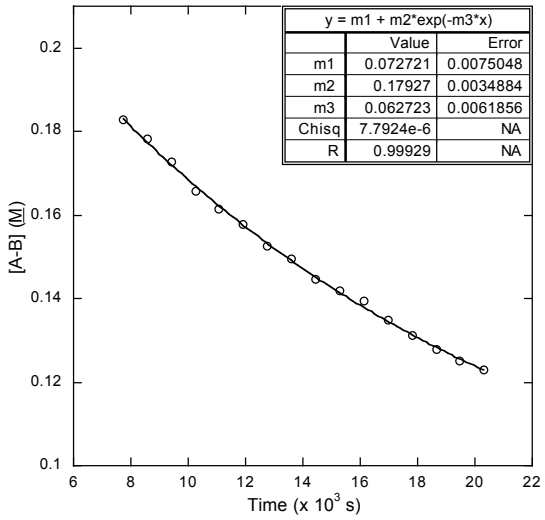

Parent conditions. k_{obs} = 6.3(6) × 10^{-5} s^{-1}

^{11}B NMR peak of **6**: -26.7 ppm

Figure S9. Top: [AB] vs. time for kinetic runs wherein BH_3·THF or THF were added to 5 mol% **12** in 2:1 diglyme/benzene-d_6 at 70 ˚C as monitored by ^{11}B NMR. Exponential coefficients in exponential decay plots represent k_{obs}. Bottom right:

Figure S10 shows an illustration of the $^{11}B\{^{1}H\}$ NMR spectrum acquired for the reaction above at 70 °C after 300 s reaction time. The peaks in this ^{11}B spectrum are **6** (-26.7 ppm), AB (-22 ppm), and $BF_3{\cdot}OEt_2$ in dyglyme co-axial external standard (0 ppm).

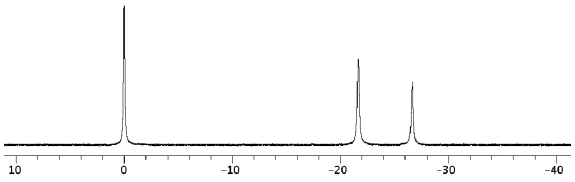

Figure S10. A representative ^{11}B NMR spectrum.

*H. Structure and Kinetic Studies of Ru-NH_3 adduct **23**.*

Ru-NH_3 adduct **23** was isolated in 59% yield.[3] ^{1}H NMR (pyridine-d_5, 600 MHz) and ^{13}C{^{1}H} NMR (pyridine-d_5, 150 MHz) are shown in Figure S11.

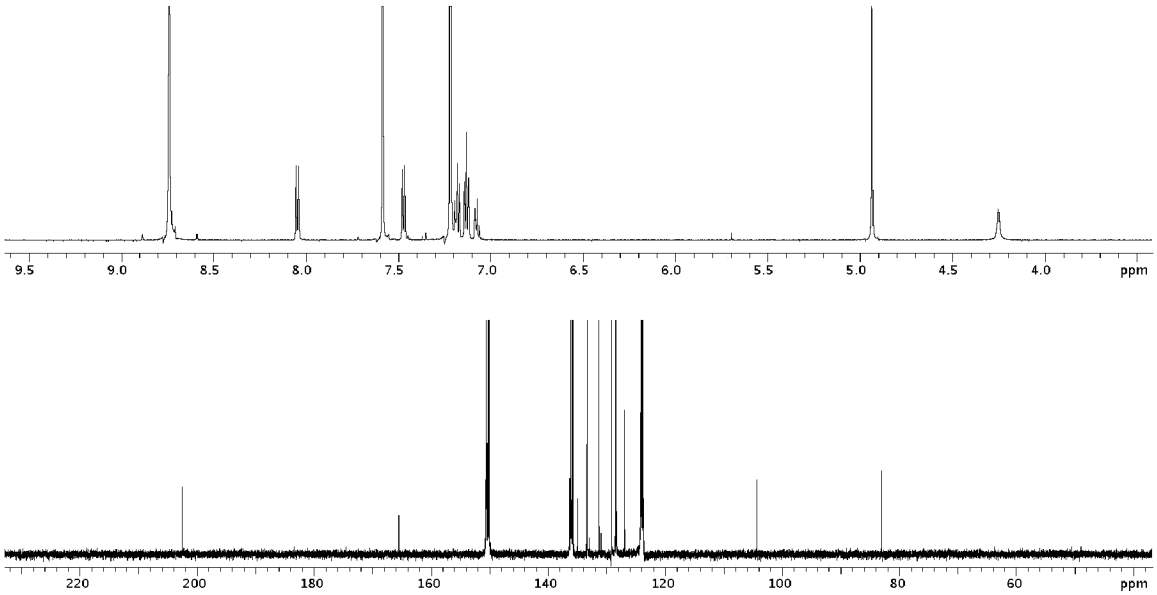

Figure S11. ^{1}H and ^{13}C NMR of **23** taken in pyridine-d_5 at 25 ˚C.

A reaction between **12** and borazine affords multiple κ^1-Ru—H complexes. Upon removal of all free borazine under vacuum, the reaction mixture was re-dissolved in benzene-d_6. The relative integrations of the κ^1-Ru—H hydride signals and the aryl region in the resulting spectrum show that the products of this reaction comprise > 90% κ^1-Ru—H complexes (Figure S12). Aqueous work-up on this sample affords **23** in 42% isolated yield. Therefore, because these κ^1-Ru—H complexes convert to **23**, they must be covalently bound to borazine, because it is the only plausible source of NH_3.

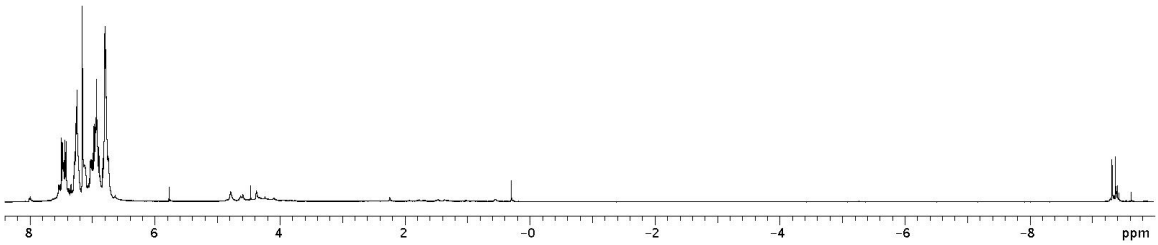

Figure S12. ^{1}H NMR taken in benzene-d_5 at 25 ˚C of a reaction between **12** and borazine after reaction completion and removal of the volatiles (mostly solvent and borazine) under vacuum.

Treatment of the data for **23**-catalyzed dehydrogenation is shown in Figure S13.

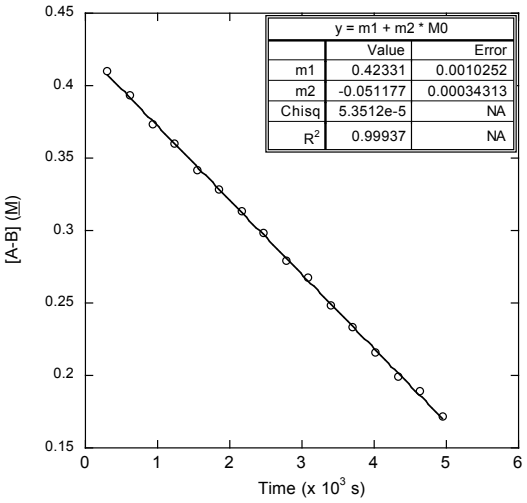

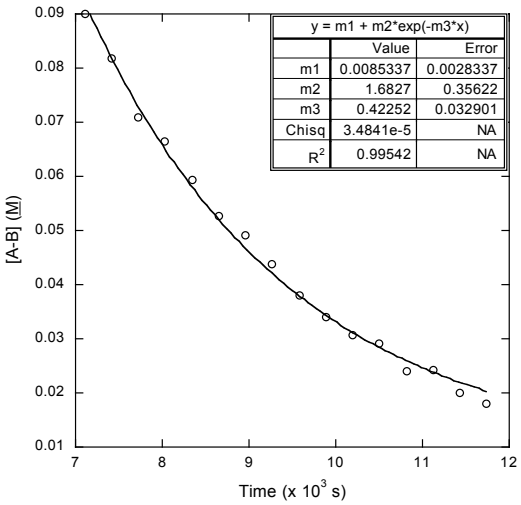

Fast catalysis, rate = $5.12(3) \times 10^{-5}$ M s^{-1} Slow catalysis case, $k_{obs} = 4.23(33) \times 10^{-4}$ s^{-1}

Figure S13. [AB] vs. time for kinetic run monitored by ^{11}B NMR with 5 mol % **23** in 2:1 diglyme/benzene-d_6 at 70 ˚C. The slope in the linear plot represents reaction rate, and the exponential coefficient in the exponential decay plot represent k_{obs}.

I. 1,10-Phenanthroline Poisoning Kinetics.

Figure S14 shows raw kinetics data for AB dehydrogenation in the presence of 0.5 and 0.1 molar equivalents 1,10-phenanthroline collected as described in the main text. A parallel run in which 7.7 mg ammonia borane (0.25 mmol) and 13.6 mg **13** (25 μmol, 10 mol % versus AB) were dissolved in 0.6 mL 2:1 diglyme/ benzene-d_6 was also conducted as a control.

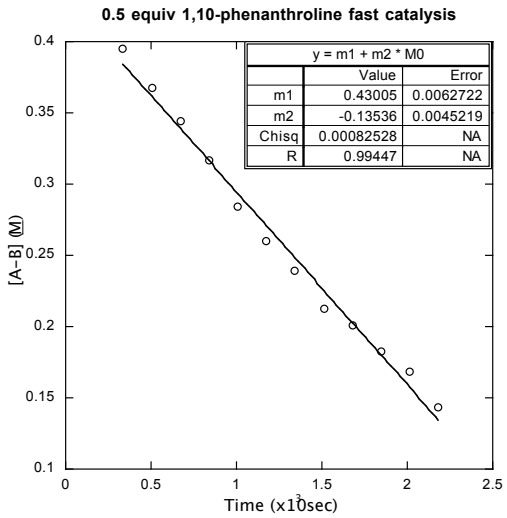

Conversion of AB in fast catalysis case: ca. 66%. Rate = 1.35 (5) × 10^{-4} M s^{-1}

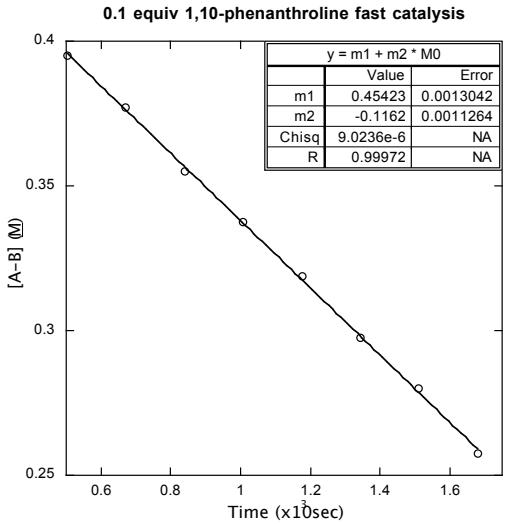

Conversion of AB in fast catalysis case: ca. 40%. Rate = 1.16(1) × 10^{-4} M s^{-1}

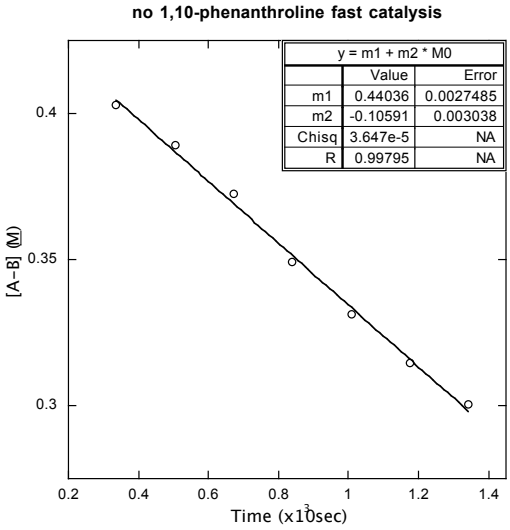

Conversion of AB in fast catalysis case: ca. 28%. Rate = 1.06(3) × 10^{-4} M s^{-1}

Figure S14. [AB] vs. time for kinetic runs monitored by ^{11}B NMR. The slope in the linear plots represents reaction rate, and the exponential coefficient in the exponential decay plots represent k_{obs}.

Scheme S2 suggests a possible explanation for observation that phenanthroline accelerates catalysis. Conceptually, we speculate that phenanthroline is protecting the reactive site on ruthenium from hydroboration. This can enable a hydrogen bond from **28**'s ligand oxygen to ammonia borane, analogous to those well documented for imine reduction with the Shvo system.[4] We suspect the reaction process is akin to **23** catalyzed ammonia borane dehydrogenation, however the equilibrium between **17** and **28** is slower (versus the equilibrium between **17** and **23**) and thus enables a faster catalysis mechanism.

Scheme S2. Proposed Mechanism of Phenanthroline Protecting **17**.

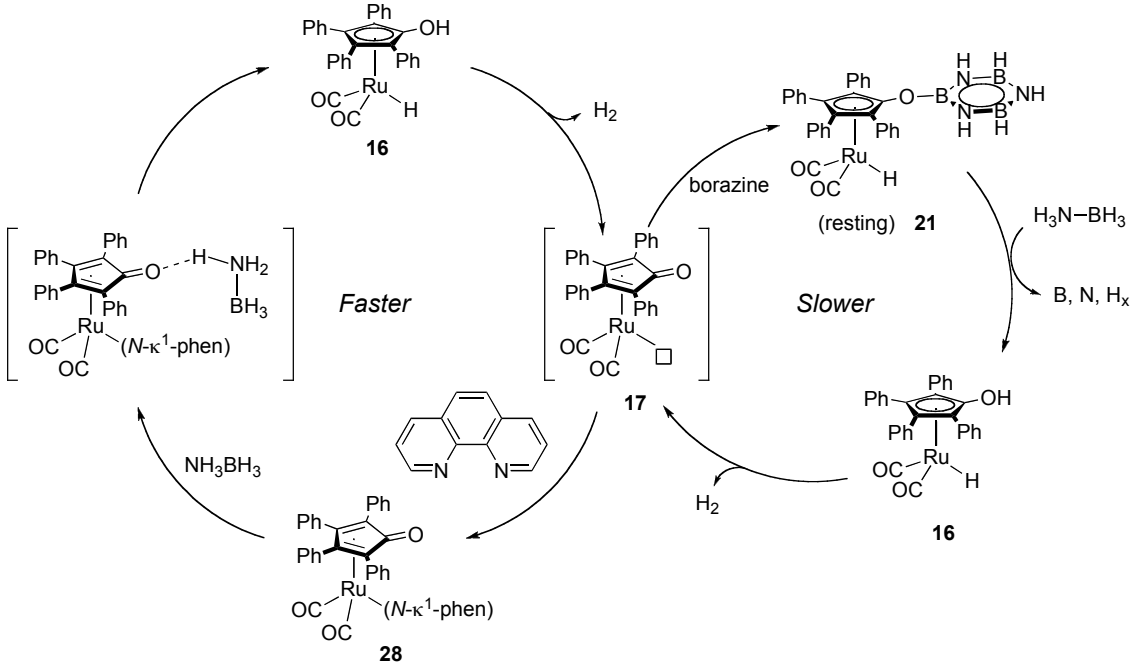

Fractional poisoning on **26**-catalyzed ammonia borane dehydrogenation with 1,10-phenanthroline was also conducted. **26** was prepared in situ by dissolving 6.8 mg **18** (12 μmol) and 1.2 μL catechol borane in a 0.6 mL 2:1 diglyme/benzene-d_6 solution and heated at 55 ˚C for 30 min. The resulting solution was checked by ^{1}H-NMR before proceeding to next step. Ammonia borane (7.7 mg, 0.25 mmol) and 2.2 mg (12 μmol, 50 mol % versus **26**) were then added to this solution and dehydrogenation was started and monitored at 70 ˚C. AB consumption throughout the duration of the reaction was determined using ^{11}B NMR and is shown in Figure S15. These data show that although the rate is not proportionally affected by the presence of phenanthroline, so the reaction is most likely homogeneous.

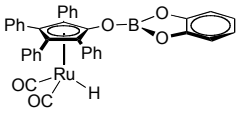

26

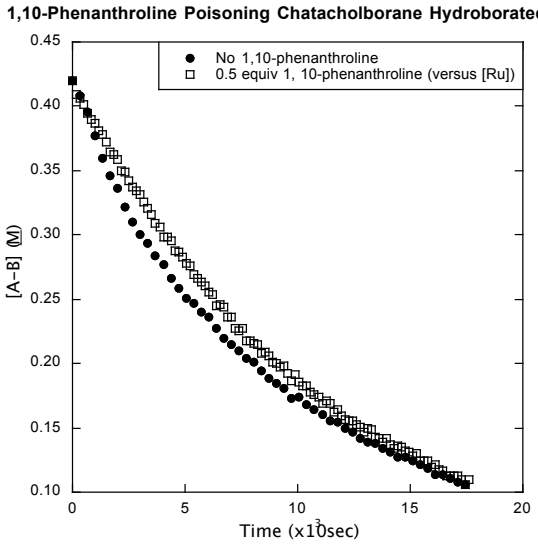

Figure S15. [AB] vs. time for kinetic runs monitored by ^{11}B NMR. 1,10-phenanthroline doesn't impact the reaction rate significantly.

IV. References

1. Wildeman, T.; Sneddon, L. G. *Inorg. Chem.* **1995,** *34*, 1002-1003.
2. Koren-Selfridge, L.; Query, I. P.; Hanson, J. A.; Isley, N. A.; Guzei, I. A.; Clark, T. B. *Organometallics* **2010,** *29*, 3896-3900.
3. Hollmann, D.; Jiao, H.; Spannenberg, A.; Bähn, S.; Tillack, A.; Parton, R.; Altink, R.; Beller, M. *Organometallics* **2009,** *28*, 473-479.
4. (a) Samec, J. S.; Éll, A. H; Åberg, J. B.; Privalov, T.; Eriksson, L.; Bäckvall, J.-E. *J. Am. Chem. Soc.* **2006**, *128*, 14293. (b) Casey, C. P.; Johnson, J. B. *J. Am. Chem. Soc.* **2005**, *127*, 1883. (c) Samec, J. S.; Éll, A. H; Bäckvall, J.-E. *Chem. Commun.* **2004**, 2748. (c) Éll, A. H; Johnson, J. B.; Bäckvall, J.-E. *Chem. Commun.* **2003**, 1652. (d) Casey, C. P.; Bikzhanova, G. A.; Cui, Q.; Guzei, I.A. *J. Am. Chem. Soc.* **2005**, *127*, 14062. (e) Casey, C. P.; Clark, T. B.; Guzei, I. A. *J. Am. Chem. Soc.* **2007**, *129*, 11821. (f) Åberg, J. B.; Bäckvall, J.-E. *Chem. Eur. J.* **2008**, *14*, 9169.